

DESIGN AND ANALYSIS OF A NOVEL 2-COLLINEAR-DOF STRUT WITH EMBEDDED ELECTROMAGNETIC SHUNT DAMPERS

27-30 September 2016, Toulouse, France

Alessandro Stabile⁽¹⁾, Guglielmo S. Aglietti⁽¹⁾, Guy Richardson⁽²⁾, Geert Smet⁽³⁾

⁽¹⁾ *Surrey Space Centre, University of Surrey, Guildford, GU2 7XH, UK, a.stabile@surrey.ac.uk*

⁽²⁾ *Surrey Satellite Technology Ltd. (SSTL), 20 Stephenson Rd, Surrey Research Park, Guildford, GU2 7YE, UK*

⁽³⁾ *ESA/ESTEC, Keplerlaan 1, PO Box 299, 2200 AG, Noordwijk, Netherlands*

ABSTRACT

This paper addresses the characterisation and analysis of a 2-collinear-DoF strut with embedded electromagnetic shunt dampers. The use of a negative resistance in the shunt circuit has been proved to considerably enhance the damping performance of this kind of electromagnetic dampers. The analytical model is reported and the theoretical results are compared with other damping methods. This work demonstrates the feasibility of achieving a remarkable decay rate of -80 dB/decade with a device that is smaller than previously-presented active struts and does not require complex electronics to operate.

1. INTRODUCTION

Micro-vibration on board a spacecraft is an important issue that affects payloads requiring high pointing accuracy such as high-resolution cameras or laser-communication systems. There are several approaches to tackle this issue, but the use of micro-vibration dampers to isolate the disturbance sources or the sensitive instruments from the satellite structure has proved to be one of the most effective methods. Several dampers have been studied and developed for micro-vibration mitigation, and they can be divided into three categories: passive (e.g. viscoelastic materials [1] and D-struts [2]), active (e.g. piezoelectric stack actuators [3] and voice coil actuators [4]) and semi-active (e.g. magnetorheological fluids and shape memory materials [5]). Among all this kind of dampers, viscoelastic materials (VEM) are the cheapest and lightest damping solutions and are widely used by companies in the space sector. Nevertheless, the several drawbacks that these materials present (e.g. the limited loss factor or the strong dependency on the operating temperature and frequency ranges) have bolstered the research on the development of damping solutions that guarantee good isolation performances in a wide temperature/frequency range.

Electromagnetic dampers have been extensively studied in the last two decades as they present several advantages over other devices, such as the contactless nature of their damping force, the simple analytical model and the possibility to use them as passive, active or semi-active dampers. In particular, by connecting a shunting circuit to the electromagnet terminals it is possible to change the device's frequency response and increase its damping performance. The use of only passive components in electromagnetic shunt dampers (EMSD) has been proved to be limited due to the off-the-shelf availability of high-value components and their inherent resistance. These limitations can be overcome through the use of negative impedances. EMSD with negative resistance applied to a 1-DoF system was proved to effectively eliminate the resonance peak and produce a roll-off slope of -40 dB/dec [6].

This paper presents a novel 2-collinear-DoF strut with embedded EMSDs. The state-space model of the system is reported, and the multiphysics finite element analysis of the EMSD in which the thermal domain is integrated with the electromagnetic and mechanical domains is presented.

Particular attention is given to the estimation of the strut damping performance throughout the operating temperatures and frequency ranges of a typical space mission. This work demonstrates the feasibility of achieving a remarkable decay rate of -80 dB/decade with a device that is smaller than previously-presented active struts (the EMSD's secondary mass is less than 4% of the supported mass) and does not require complex electronics to operate.

2. ELECTROMAGNETIC SHUNT DAMPER

An EMSD is a self-excited device that provides a reaction force proportional to the relative velocity between the electromagnet and the permanent magnet. This motion induces an electromotive force V_0 (i.e. electric voltage) at the terminals of the electromagnet that can be expressed with the Faraday-Lenz law:

$$V_0 = \oint (\vec{v} \times \vec{B}) \cdot d\vec{l} = K_d v_z \quad (1)$$

where v_z is the component of the relative velocity along the electromagnet-magnet coaxial longitudinal axis and K_d is defined as the electro-mechanical transducer coefficient. K_d can be simplified with the assumption of micro-vibration load case (i.e. relative displacement in the order of tenths of a millimetre) with the expression:

$$K_d = 2\pi n_t r_{avg} \bar{B}_r \quad (2)$$

where n_t is the number of turns of the coil, r_{avg} is the average radius of the conductor, and \bar{B}_r is the average radial component of the magnetic field through the coil cross section.

The electric voltage V_0 produces a current, I , that flows in the closed circuit made by the electromagnet and the shunt circuit. Once the induced current is generated, it couples with the surrounding magnetic field to produce the Lorentz force. This force is described by the equation:

$$\vec{F}_d = \oint I d\vec{l} \times \vec{B} = -K_d I \hat{z} \quad (3)$$

These two laws (Eq. 1 and 3) considered together demonstrate that the force produced by a permanent magnet which moves close to a conductive material is proportional in magnitude and opposite in direction to their relative velocity, thus behaving similarly to a viscous damper. By using a negative resistance in the shunt to reduce the overall resistance it is possible to increase the current flowing in the circuit and hence improve the damping performance. In this study, the negative resistance is created by utilising an analogue circuit called negative impedance converter. It consists of a single operational amplifier (op-amp) and three resistors that are connected as shown in Fig.1. The equivalent resistance of the shunt is:

$$R_s = -R_x \left(\frac{R_z}{R_y} \right) \quad (4)$$

Although the shunt circuit requires power to operate, this type of EMSD can be considered as a semi-active damper because the negative resistance acts as a passive electrical component having a constant negative magnitude, without requiring any control algorithm, and also because it needs little power (in the order of tenths of Watts) to operate. The correctness of these assumptions and the good correlation between the analytical model and the test results were verified in [6] where the proposed EMSD was applied to a single-DoF system.

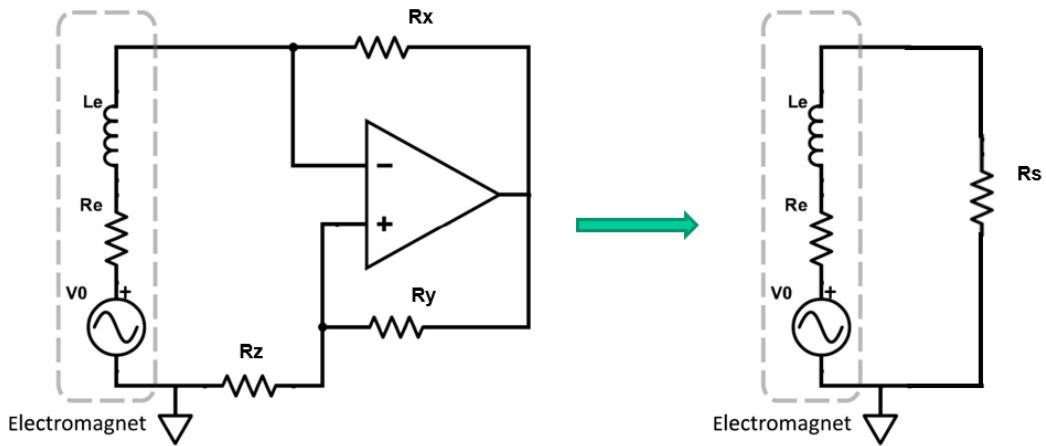


Fig. 1. Left-hand-side: electrical schematic of the negative resistance converter connected to the electromagnet. Right-hand-side: the equivalent circuit schematic where the negative resistance is represented by a passive resistor having negative magnitude.

3. 2-COLLINEAR-DOF STRUT MODELLING

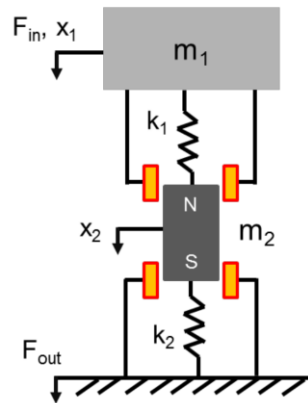


Fig. 2. Schematic representation of the 2-collinear-DoF model

The system presented in this paper is made of two collinear degrees of freedom. The magnet mass m_2 is connected to the supported mass m_1 and to the ground via two separate springs, as it can be seen from Fig.2, and the two masses can only move along their longitudinal axis. By exploiting the two poles of the magnet, two separate coils can be rigidly connected respectively to the suspended mass and the ground thus producing two levels of damping. The suspended mass has been chosen to be 5 kg and corresponds approximately to the mass of two 100SP-O reaction wheels used by Surrey Satellite Technology Ltd (SSTL). Through the assumptions of micro-vibration and steady-state conditions, this system can be modelled via a state-space representation. The state vector consists of six state variables: displacement (x_1, x_2) velocity (\dot{x}_1, \dot{x}_2) and circuit current (I_1, I_2) . The state space model can be written as:

$$\begin{bmatrix} \dot{x}_1 \\ \dot{x}_2 \\ \ddot{x}_1 \\ \ddot{x}_2 \\ \dot{I}_1 \\ \dot{I}_2 \end{bmatrix} = \begin{bmatrix} 0 & 0 & 1 & 0 & 0 & 0 \\ 0 & 0 & 0 & 1 & 0 & 0 \\ -k_1/m_1 & k_1/m_1 & 0 & 0 & -K_d/m_1 & 0 \\ k_1/m_2 & -(k_1+k_2)/m_2 & 0 & 0 & K_d/m_2 & -K_d/m_2 \\ 0 & 0 & K_d/L_1 & -K_d/L_1 & -R_1/L_1 & 0 \\ 0 & 0 & 0 & K_d/L_2 & 0 & -R_2/L_2 \end{bmatrix} \begin{bmatrix} x_1 \\ x_2 \\ \dot{x}_1 \\ \dot{x}_2 \\ I_1 \\ I_2 \end{bmatrix} + \begin{bmatrix} 0 \\ 0 \\ 1/m_1 \\ 0 \\ 0 \\ 0 \end{bmatrix} F_{in} \quad (5)$$

$$Y = [0 \quad k_2 \quad 0 \quad 0 \quad 0 \quad K_d] \begin{bmatrix} x_1 \\ x_2 \\ \dot{x}_1 \\ \dot{x}_2 \\ I_1 \\ I_2 \end{bmatrix} + [0] F_{in} \quad (6)$$

where R_1 and L_1 are the circuit features associated with the top coil, whereas R_2 and L_2 are associated with the bottom coil. Also, R_1 and R_2 are obtained by summing the coil resistance, R_e , with the shunt negative resistance, R_s . The output vector Y represents the force transmitted to the ground.

The environmental conditions at which a satellite operates can usually affect the performance of dampers (e.g. VEMs are strongly dependent on the surrounding temperature). The typical operating range of a reaction wheel is from -20°C to $+50^\circ\text{C}$. The proposed damper has been designed to provide good micro-vibration isolation within the operational temperature range without requiring any active control. A parametric trade-off has been conducted in order to meet the following goals throughout the whole temperature range of interest:

- Maximum amplification below 6 dB
- Corner frequency at 10 Hz or below
- At least -40 dB at 100 Hz.

This system presents several parameters (both electrical and mechanical) that could be tuned to modify its dynamic response. To simplify the analysis, it was assumed that the two springs were identical ($k_1 = k_2$), as well as the electrical properties of the two electromagnetic circuits ($R_1=R_2$ and $L_1=L_2$). In terms of temperature dependency, only the coil resistance, R_e , and the magnet residual induction (i.e. the electro-mechanical coefficient, K_d) are notably affected by the temperature change. In particular, the copper resistivity of the coils increases linearly with respect to the temperature with a thermal coefficient of $0.00386 \text{ }^\circ\text{C}^{-1}$, whereas the residual induction of the Nd-Fe-B magnet is characterised by a linear temperature coefficient of $-0.0012 \text{ }^\circ\text{C}^{-1}$. These two effects have been taken into account for the assessment of the damper performance. Regarding the negative resistance circuit, the three resistors R_x , R_y and R_z can be chosen among space-qualified, off-the-shelf components that have tolerances down to 0.005% and temperature coefficients of $10^{-6} \text{ }^\circ\text{C}^{-1}$. Hence, these resistors can be considered constant over a wide temperature range when compared with the electromagnet resistance. The outcome of the parametric trade-off is reported in Tab.1.

It is important to notice that the chosen Nd-Fe-B magnet has a mass of 180 g, which corresponds to less than 4% of the suspended mass. In terms of stability, the EMSD would become unstable if the total resistance (R_e+R_s) is negative, and this could happen at the lowest temperature range limit (where R_e reaches its minimum value). For this reason, during the parametric trade-off a minimum value of 0.2Ω was imposed on the total resistance at a temperature of $-20 \text{ }^\circ\text{C}$.

Tab. 1. Final choice of the parameter set obtained through a trade-off

Property	Value			
Suspended mass, m_1 (kg)	5			
Magnet mass, m_2 (kg)	0.18			
Spring stiffness, $k_1=k_2$ (N/m)	2000			
Coil Inductance, $L_1=L_2$ (mH)	8			
Shunt resistance, R_s (Ω)	-3.0			
	Temp.	-20°C	15°C	50°C
Coil resistance, R_e (Ω)		3.20	3.65	4.10
E-m Transducer coefficient, K_d (N/A)		11.28	10.79	10.29

4. FREQUENCY-DOMAIN ANALYSIS

The use of state space modelling considerably simplifies the analysis of the system in the frequency domain into which it can be converted by taking the Laplace transform. The transfer function between the input force, F_{in} , and the force transmitted to the ground, Y , can be observed in Fig.3. For simplicity, only the system dynamic responses at three different temperatures (-20 °C, +50°C and the range mid-point, +15 °C) have been reported, and they have been compared with a similar system without EMSD. From Fig.3 it can be seen that: the amplification at the resonance frequency is always kept below 6dB, the corner frequency does not exceed 10 Hz and the attenuation at 100 Hz is greater than 40dB. Therefore, the three requirements outlined in the previous section have all been met.

The important contribution of using the negative resistance can also be seen in the system response to a step function when compared with the same system without EMSD (only a small amount of inherent mechanical damping has been included). From Fig.4 it can be observed how the proposed damper quickly suppresses undesired oscillations and reaches the steady state conditions in less than a second. This plot allows also to easily quantify the amount of damping introduced with the EMSD in relation to the system's critical damping. In particular, the damping ratio (defined as the actual damping divided by the critical damping) of the system under examination varies from 0.3 to 0.45 within the temperature range of interest.

The 2-collinear-DoF damper presented in this paper shows good advantages in terms of micro-vibration attenuation even when compared to other damping solutions. The transfer function of the system under examination (at the temperature of 15 °C) is reported in Fig.5 along with the transfer function of a 1-DoF system with EMSD [6] and the one of a VEM passive isolator [7]. In particular, the 2-collinear-DoF system is capable of producing a better micro-vibration attenuation in comparison with the other two systems for almost the entire frequency spectrum. Moreover, the EMSD almost completely eliminates the resonance peak that is characteristic of a VEM isolator and presents a final slope that is 40dB/dec greater than the one showed by the 1-DoF system.

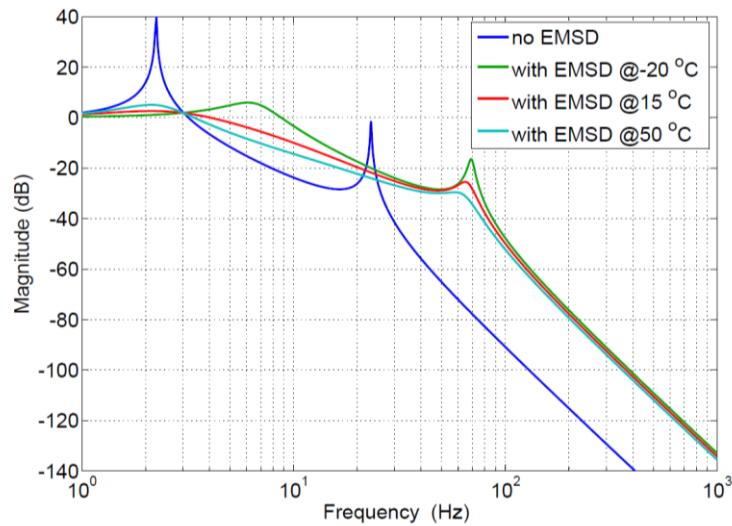


Fig. 3. Comparison of the force transfer functions between the system without EMSD and the system with EMSD at three different temperatures

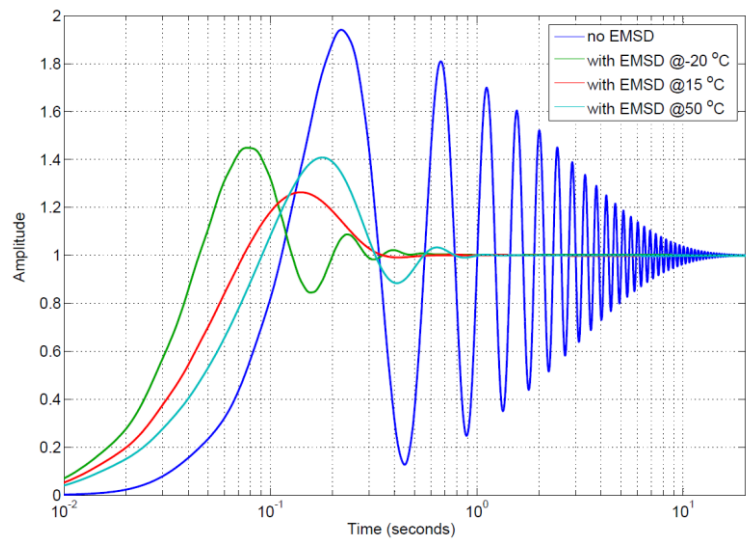


Fig. 4. Comparison of the step responses between the system without EMSD and the system with EMSD at three different temperatures

The proposed strut shows several advantages also in comparison to active dampers. Active control methods are typically characterised by complex, cumbersome electronics that considerably affects the overall mass of the isolation system (e.g. the hexapod presented in [8] has an electronics mass of 9kg which corresponds to 72% of the overall hexapod mass) and require a significant amount of power to drive actuators and sensors (e.g. the single strut in [3] needs a minimum of 15W to operate). Contrarily, the 2-collinear-DoF strut uses small circuit boards composed by few electric parts that require less than 0.5 W to produce the high damping performance reported in this paper. The next phase of this project will aim at corroborating the analytical results presented in this paper with a test campaign. The test rig has been designed and assembled on a Kistler table, and it can be seen in Fig.6.

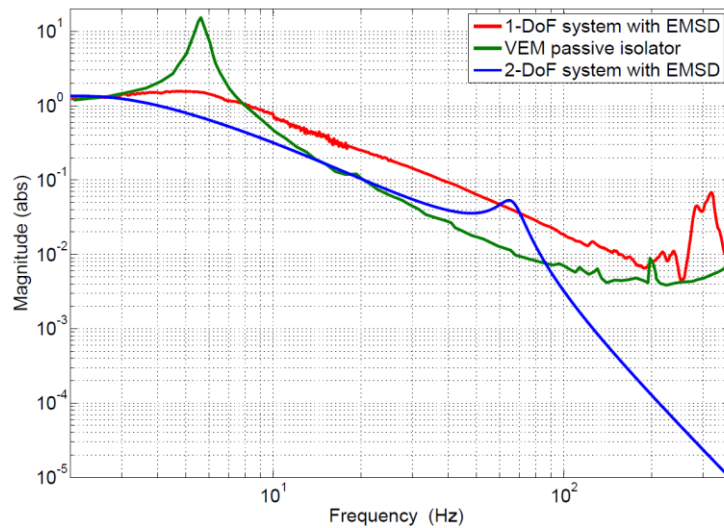


Fig. 5. Comparison of the force transfer functions between three different damping systems: (red) test result from 1-DoF system with EMSD [6]; (green) test result from VEM passive isolator [7]; (blue) analytical data from 2-collinear-DoF system with EMSD at 15°C

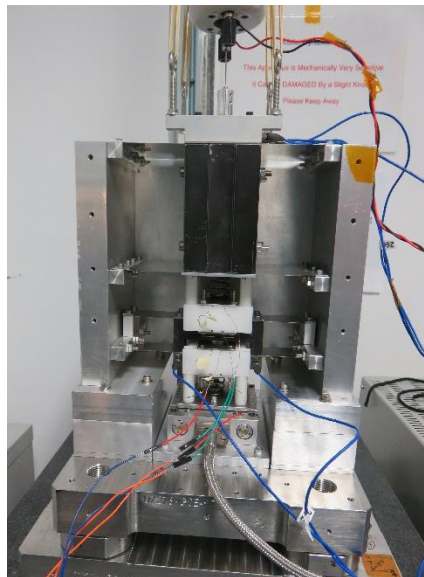


Fig. 6. Experimental test rig mounted on the Kistler table

5. CONCLUSIONS

The objective of the present paper was to create and validate the analytical model of a novel 2-collinear-DoF system and to assess the improved damping performance of this system when compared to other damping solutions. The better isolation of the proposed damper was achieved through the use of negative-resistance analogue circuits to reduce the inherent resistance of the electromagnetic coils. This work demonstrates the feasibility of achieving an almost completely elimination of the resonance peak and a remarkable decay rate of -80dB/dec throughout the whole temperature range of interest. The proposed damper shows several advantages with respect to both passive isolators (in terms of micro-vibration mitigation performance) and active dampers (cumbersome electronics increase the overall mass of the isolators). The 2-collinear-DoF strut presented in this paper does not require a control algorithm to operate and uses a small secondary mass (less than 4% of the suspended mass) and a simple, highly robust circuit board, which will

make this damper an interesting competitor with respect to other well-established damping solutions for future space applications.

6. REFERENCES

- [1] G. Richardson, G. Smet and G. Aglietti, "managing micro-vibration on the sst1300-s1 a 400 kg 1m resolution earth imaging spacecraft", in *13th European Conference on Spacecraft Structures, Materials and Environmental Testing (SSMET)*, 2014.
- [2] P. Davis, D. Carter and T. Hyde, "Second generation hybrid d-strut", in *SPIE Smart structures and material conference*, 1995.
- [3] E. Anderson, J. Fumo and R. Erwin, "Satellite ultraquiet isolation technology experiment (suite)", in *Aerospace Conference IEEE*, 2000.
- [4] A. Preumont, M. Horodinca, I. Romanescu, B. de Marneffe, M. Avraam, A. Deraemaeker, F. Bossens and A. Abu Hanieh, "A six-axis single-stage active vibration isolator based on Stewart platform", *Journal of Sound and Vibration*, vol. 300, no. 3-5, pp. 644-661, 2007.
- [5] C. Liu, X. Jing, S. Daley and F. Li, "Recent advances in micro-vibration isolation", *Mechanical Systems and Signal Processing*, vol. 56-57, pp. 55-80, 2015.
- [6] A. Stabile, G. Aglietti, G. Richardson and G. Smet, "Design and verification of a negative resistance electromagnetic shunt damper for spacecraft micro-vibration", *Journal of sound and vibration (UNDER REVIEW)*.
- [7] R. Bronowicki, A. MacDonald, Y. Gursel, R. Goullioud, T. Neville and D. Platus, "Dual stage passive vibration isolation for optical interferometer missions", in *SPIE Interferometry in space*, 2003, pp. 753-763.
- [8] J. Jacobs, J. Ross, S. Hadden, M. Gonzalez, Z. Rogers and B. Henderson, "Miniature vibration isolation system for space applications - phase II", in *SPIE Smart Structures and Materials*, 2004.